

Spectral dependences of the activity and selectivity of N-doped TiO₂ in photodegradation of phenols

A.V. Emeline¹, X. Zhang, M. Jin, T. Murakami, A. Fujishima*

Kanagawa Academy of Science and Technology, Kawasaki, Kanagawa, Japan

ARTICLE INFO

Article history:

Available online 14 January 2009

Keywords:

Photocatalysis
Visible-light photocatalyst
Quantum yield
Selectivity
Doping

ABSTRACT

In present study we report the spectral dependencies of the quantum yield of phenol and 4-chlorophenol photodegradation over N-doped TiO₂ and the selectivity of the photocatalyst toward formation of the major intermediates. Applying the theoretical model developed earlier [A.V. Emeline, V.K. Ryabchuk, N. Serpone, J. Phys. Chem. B. 103 (1999) 1316; A.V. Emeline, A.V. Frolov, V.K. Ryabchuk, N. Serpone, J. Phys. Chem. B 107 (2003) 7109] for analysis of the experimental spectral dependencies we conclude that extrinsic N-doped induced absorption is formed by overlapping of several single absorption bands, which presumably correspond to different intrinsic defects (color centers) in TiO₂ distinguished by different efficiency of photogeneration of charge carriers. It is also inferred that measurement and corresponding analysis of spectral dependencies of the quantum yield and selectivity of heterogeneous photochemical reactions can be considered as a powerful spectroscopic mean to deconvolve the complex non-resolved absorption spectrum of solids.

© 2009 Elsevier B.V. All rights reserved.

1. Introduction

One of the major parameters characterizing the activity of a photocatalyst in heterogeneous systems is the quantum yield of a surface photochemical process. It is defined as the ratio between the number of species (molecules, ions) chemically transformed per unit time and the number of absorbed photons per unit time as expressed by Eq. (1) [1,2],

$$\Phi = \frac{dN_m/dt}{dN_{hv}/dt} \quad (1)$$

where N_m is the number of molecules (ions) chemically transformed, and N_{hv} is the number of absorbed photons of monochromatic light, $h\nu$. The importance of the quantum yield as a characteristic of the photocatalyst activity is that absorbed light only can initiate the surface photochemical transformation. Thus, the quantum yield of a surface photochemical process characterizes the ability of a photocatalyst to convert the light absorbed to an interfacial chemical transformation in heterogeneous system.

The intriguing feature of the quantum yield of an interfacial process is the alteration of this parameter with the wavelength of photoexcitation, that is, a spectral dependence of the quantum yield experimentally observed for different heterogeneous systems

[3–10]. A one-dimensional model reported earlier [11,12] indicates that the quantum yield of an elementary chemical transformation occurring on a photocatalyst surface can be represented by Eq. (2) provided that the rate of the surface photoprocess is independent of reagent concentration,

$$\Phi = \frac{k_{tr} S_0 \chi \alpha L^2}{D(\tanh(d/2L) + \xi)(1 - \alpha^2 L^2)} \left(\tanh\left(\frac{d}{2L}\right) \coth\left(\frac{\alpha d}{2}\right) - \alpha L \right) \quad (2)$$

where k_{tr} is the rate constant of charge carrier trapping by surface active center (S_0), D is the diffusion coefficient of charge carrier migration, ξ is the ratio between the surface and bulk recombination of the charge carriers, d is the one-dimensional size of the photocatalyst crystal, L is the diffusion length of the charge carrier, χ is the quantum yield of internal photoeffects, generally a constant within a single absorption band, and α is the absorption coefficient of the photocatalyst specimen. Consequently, within a single absorption band, corresponding to a given mechanism of solid photoexcitation, the spectral variation of the quantum yield is dictated by alteration of the absorption coefficient of the photocatalyst and corresponding dimensionless ratios, e.g. αL , αd and $d/2L$ that reflect the interplay between the spatial distributions of the photogeneration of charge carriers and their probability to reach the surface.

However, according to Eq. (2), such spectral dependence of the quantum yield is well pronounced only in the case of strong light absorption when $\alpha L \gg 1$, $\alpha d \gg 1$. Otherwise, for $\alpha L \ll 1$ and $\alpha d \ll 1$

* Corresponding author.

E-mail address: fujishima@newkast.or.jp (A. Fujishima).

¹ Permanent address: Department of Photonics, V.A. Fock Institute of Physics, St.-Petersburg State University, St.-Petersburg, Russia.

Eq. (2) can be simplified to:

$$\Phi = \frac{k_{tr} S_0 \chi L^2}{Dd} \left\{ \frac{\tanh(d/2L)}{\tanh(d/2L) + \xi} \right\} \neq f_n(\alpha) \quad (3)$$

where the quantum yield does not depend on the absorption coefficient and on its spectral variation within a *single* absorption band, and therefore becomes spectrally independent. The latter scenario, in particular, corresponds to photoexcitation of nanoparticles ($\alpha d \ll 1$) and to photoexcitation within the spectral region of extrinsic light absorption.

At the same time, one should note that light absorption by solids is practically always complex and is formed by the overlap of different single absorption bands that correspond to different mechanisms of photoexcitation of the solids characterized by different quantum yields of internal photoeffects, χ . In such a case of complex light absorption the quantum yield of interfacial photoreaction can be represented by Eq. (4) (for details see [10,11]). Consequently, according to Eqs. (1) and (3) for each single absorption band the partial reaction rate can be expressed as:

$$\Phi = \frac{\sum_i R_i}{\rho \sum_i A(\lambda)_i} = \frac{\text{const} \sum_i \chi_i A(\lambda)_i}{\sum_i A(\lambda)_i} \quad (4)$$

where χ_i is the quantum yield of internal photoeffects, $A(\lambda)_i$ is the absorbance of the *i*th single absorption band, and ρ is the photon flow of the actinic light at the given wavelength λ . The total reaction rate, R , at a given wavelength is represented by Eq. (5),

$$R = \sum_i R_i = \text{const} \rho \sum_i \chi_i \times A(\lambda)_i \quad (5)$$

Since a quantum yield of the internal photoeffects (χ) is a unique parameter for each single absorption band, the quantum yield of the surface photoreaction becomes spectrally dependent and its spectral behavior is sensitive to the degree of overlap and to the type of single absorption bands that compose the absorption spectrum of the solid. In other words, the shape of the spectral dependence of the quantum yield is sensitive to the composition of the absorption spectrum of a solid photocatalyst. As a result, the quantum yield is constant within a single absorption band, whereas the band-like or step-like shape of the spectral dependence of the quantum yields indicates the overlap of a chemically active light absorption band with less active or inactive light absorption bands [7,11]. Concomitantly, such spectrally dependent measurements can be considered as a certain type of spectroscopy, which allows the determination of the spectral features in the absorption spectrum of the photocatalyst that are responsible for the photochemically active light absorption. Hence, the spectral dependence of the quantum yield allows for the resolution of the broad absorption envelope in the absorption spectrum of the photocatalyst and for the selection of certain overlapping single absorption bands that, when convolved, form the absorption spectrum.

Another significant feature of the behavior of heterogeneous photochemical system is the variation of the selectivity of the photocatalyst with the alteration of the wavelength of photoexcitation, that is, spectral selectivity [3,9,13]. Selectivity, S_i , characterizes the ability of photocatalyst to drive the heterogeneous photoreaction toward a certain reaction pathway and can be determined as the ratio between the number of molecules of a given reaction product formed, N_i , and the number of molecules of reagent consumed, N_r , during photoreaction

$$S_i = \frac{dN_i/dt}{dN_r/dt} \quad (6)$$

Generally, there exist two reasons for the experimental observation of the spectral dependence of photocatalyst selectivity:

kinetic and thermodynamic. The former one is the spectral variation of the ratio between the surface concentrations of electrons and holes, e_s/h_s , which results in different probability of reduction and oxidation pathways. In turn, spectral alteration of the ratio e_s/h_s in the case of non-uniform bulk photoexcitation of the photocatalyst, depends on the different probabilities for electrons and holes to reach the surface and further participate in surface chemical transformations with alteration of absorption coefficient of photocatalyst [11–13]. Otherwise, in the case of uniform bulk photoexcitation, the ratio e_s/h_s becomes spectrally dependent due to a difference in quantum yields of internal photoeffects of electron and hole photogeneration for different single absorption bands forming the convoluted absorption spectrum of the photocatalyst.

The thermodynamic reason for spectral selectivity is the possibility of generation of different surface active states at different wavelengths of photoexcitation possessing different activities (selectivity) toward the formation of different reaction products. Typically, this effect is observed for localized photoexcitation of surface states of the photocatalyst.

Promising results in extending the activity of metal-oxide photocatalysts to the visible spectral region in heterogeneous photocatalysis have been obtained recently with non-metal doping of such photocatalysts as TiO₂. In particular, a successful candidate for a photocatalyst that is sensitive to visible-light activation is N-doped TiO₂ [14–24]. In this regard, a lively debate has ensued in the recent literature [16,21,23,25–29] that has centered on the causes that lead the absorption onset of TiO₂ to be shifted to the visible region. The discussion mainly concerns the types of states and the mechanisms of photoexcitation, which are responsible for visible-light photoactivity of doped photocatalysts. One point of view states that N-doping results in band gap narrowing [14] or that the formation of dopant delocalized band states within the band gap of TiO₂ thereby increasing the photoactivity in the visible-light region. Other points of view [16,18,21,23,25] however, have proposed that such red-shifts of the absorption edge in doped TiO₂ involves electronic transitions from localized band gap states to the conduction band (CB) of the metal oxide. In turn, there is a disagreement regarding the type of these localized states: N-states vs. N-doped induced intrinsic defects of TiO₂ (such as anion vacancies or Ti³⁺ states) formed as a result of compensation of the excessive charge of N³⁻ anions [25,27,29]. The latter point of view is particularly supported by experimental results obtained in recent studies of spectral dependences of the quantum yield of oxygen and hydrogen photostimulated adsorption on N-doped TiO₂ [10].

In the present article we report measurements of the spectral dependences of the quantum yield and selectivity of N-doped TiO₂ in photodegradation of phenol and 4-chlorophenol to further clarify the possible origin(s) of this controversial issue, i.e. the absorption red-shifts.

2. Experimental

The powdered N-doped titanium dioxide specimen examined was the TP-S201 product obtained from Sumitomo Chemical Ltd., Japan and used without pre-treatment. According to the sample description presented by Sumitomo Chemical Ltd. its specific surface area is 140 m² g⁻¹; the average crystallite size is ~12 nm. X-ray diffraction structural methods confirmed the structure of TiO_{2-x}N_x sample to be anatase, whereas X-ray photoelectron spectroscopic data revealed the presence of interstitial nitrogen in the TiO_{2-x}N_x specimen and the existence of Ti–N bonds [10,30].

Distilled phenol and 4-chlorophenol (Aldrich; purity >99%) were used as reagents. Water solutions were prepared with ultrapure water (Mili-Q). The pH of the system was adjusted to pH 3 with HCl. Initial concentrations of reagents were chosen to be 1.0 mM/l to insure independence of the reaction rate of reagent concentration

and its linear dependence on light intensity (for details on necessary conditions to measure the quantum yield of heterogeneous photochemical process see [3,7,10,30]). Black body like photochemical reactor was applied to measure the spectral dependences of the quantum yield (detailed description of this type reactor can be found elsewhere [30]). TiO_2 loading (10 g/l) used in our experiments satisfied the conditions of nearly complete absorption of light by heterogeneous system at all wavelengths of photoexcitation (see [30]).

A 1000 W Xe–Hg lamp (Oriel) in combination with an IR water filter connected to a monochromator (Corner Stone, Oriel) was used as the light source. The width of the slits provided spectral resolution of about 10 nm. The optical fiber was connected to the output slit of the monochromator through a light-focusing adapter. A set of neutral density filters (Oriel) was used to vary the light intensity of the actinic light to confirm the linear dependence of the reaction rates on light intensity. Filters were placed between the output slit of the monochromator and the optical fiber. The concentrations of phenols and major reaction intermediates in the system during photoreaction were measured by HPLC methods (Shimadzu LC 2010) after filtering a 1-ml solution through an inorganic 0.02- μm membrane filter (Whatman).

Experimental errors in the measurements of the quantum yields caused by the reproducibility of the reaction rate measurements did not exceed $\sim 15\%$.

3. Results and discussion

A set of preliminary experiments to establish the required experimental conditions was run before starting the measurements of the spectral dependences of the quantum yields and selectivity. The required conditions are: independence of the quantum yield of reagent concentration and light intensity [30]. Due to interdependence of the reaction rate on both reagent concentration and light intensity [31] both conditions can be satisfied at the same time. It was found that at initial concentration of reagents 1 mM the rate of phenol(s) photodegradation does not depend on reagent concentration and scales linearly with light intensity. Therefore, both conditions were satisfied in our experiments.

Phenol and 4-chlorophenol were selected as test molecule reagents because of the difference in mechanisms of their photodegradation: the major pathway for phenol photodegradation is its photooxidation while both photoreduction and photooxidation are effective pathways of 4-chlorophenol photodegradation. This difference allows monitoring the efficiency of photoprocesses involving surface photoelectrons and photoholes (see below).

To measure the spectral dependences of the quantum yield and selectivity one needs to have the reproducible state of photocatalyst at all wavelengths. Obviously, the only available reproducible state of photocatalyst is its initial state. Consequently, all measurements of the quantum yield and selectivity were done on the basis of the initial rates of phenol(s) degradation and formation of intermediate products.

3.1. Spectral dependence of the quantum yield

Experimental spectral dependences of the quantum yields of photodegradation of phenol and 4-chlorophenol are presented in Fig. 1. As is evident from presented data, the spectral dependencies of the quantum yield demonstrate complex multi-band structure. To analyze these dependencies it is wiser to consider the spectral region of the strong fundamental absorption of TiO_2 and the spectral region of the weak extrinsic N-doped induced absorption separately.

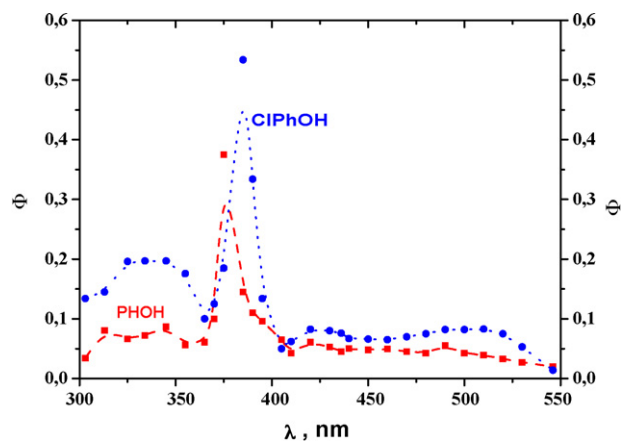


Fig. 1. Spectral dependencies of the quantum yield of photostimulated degradation of phenol and 4-chlorophenol at N-doped TiO_2 surface.

Spectral dependencies of the quantum yield of phenol photodegradation over N-doped TiO_2 in the fundamental absorption spectral region corresponds well to the spectral dependencies of different photoprocesses (including phenols photodegradation) on the pristine TiO_2 [8,32]. Two maxima in spectral dependencies (at ~ 385 nm and at ~ 335 nm) conform to energies of indirect and direct band-to-band transitions, respectively in TiO_2 indicating that no significant changes in band structure of TiO_2 that might affect the spectral dependence of the quantum yield are induced by N-doping. Although the fundamental absorption of TiO_2 is strong with absorption coefficient being as high as 10^4 cm^{-1} for indirect transition to 10^6 cm^{-1} for direct transition, because of the small size of the sample crystallites (~ 12 nm), the bulk photoexcitation of N-doped TiO_2 particles is rather uniform for absorption corresponding to indirect transitions, that is $\alpha d \ll 1$ in Eq. (2). At the same time for the spectral region corresponding to energies of direct transitions the latter condition is clearly failed. Therefore, the observed spectral dependence of the quantum yield within the spectral region of fundamental absorption results (according the Eq. (4)) from the overlapping of light absorption corresponding to indirect and direct electron band-to-band transitions characterized by different values of the quantum yield of internal photoeffect, χ . Also one may expect to observe the effect of difference in mobilities and lifetimes for charge carriers generated due to direct and indirect transitions on the spectral variation of the quantum yield (see Eq. (2)).

The most intriguing feature of the experimental spectral dependencies of the quantum yield is their behavior within the spectral region of the extrinsic N-doped induced absorption (Fig. 2). Note, that this extrinsic absorption is weak and therefore the uniform excitation of the particle bulk must be considered, that is $\alpha d \ll 1$ in Eq. (2). In other words, the spectral dependence of the quantum yield of surface photoreaction should be independent of the wavelengths of photoexcitation provided that the mechanism of photoexcitation is the same within the N-doped induced absorption. Obviously, the experimental data show the different behavior demonstrating the multi-band structure, which implies that the N-doped induced absorption band possesses the complex structure formed by overlapping of several single absorption bands characterized by different values of the quantum yields of internal photoeffect in accordance with Eq. (4).

It is also important to note that the spectral behavior of the quantum yields of phenol and 4-chlorophenol photodegradation is quite different. This difference is caused by a distinction in the mechanisms of photodegradation of the two reagents. Both oxidation and reduction pathways are significant for 4-chlorophenol degradation,

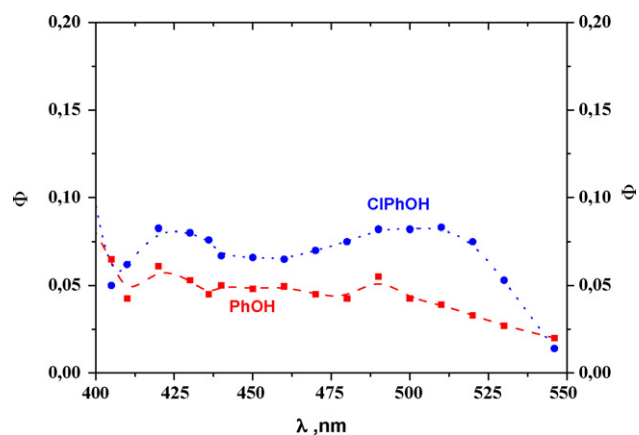


Fig. 2. Spectral dependencies of the quantum yield of photostimulated degradation of phenol and 4-chlorophenol at N-doped TiO₂ surface within the visible spectral range corresponding to N-doping induced absorption.

that is, both electron and hole photogenerated surface states participate in the process, while phenol photodegradation occurs through the oxidation pathway only by interaction of phenol molecules with hole surface states (OH-radicals) [13,33,34].

Accordingly, the expression for the rate of phenol photodegradation can be written as:

$$\frac{dC_{PhOH}}{dt} = k'_h h [PhOH] \quad (7)$$

While the rate of 4-chlorophenol photodegradation can be represented as:

$$\frac{dC_{ClPhOH}}{dt} = (k_e e + k_h h) [ClPhOH] \quad (8)$$

Consequently, the ratio between the rates of 4-chlorophenol and phenol photodegradation results in equation, considering that the rate constants of OH-radical attack on phenol and 4-chlorophenol are very similar [33,35]:

$$\frac{\Phi_{ClPhOH}}{\Phi_{PhOH}} = \frac{\{k_e e + k_h h\} [ClPhOH]}{k'_h h [PhOH]} \approx \frac{k_e e}{k'_h h} + \frac{k_h}{k'_h} \approx \text{const} \frac{e}{h} + 1 \quad (9)$$

Thus, the spectral variation of the ratio between the quantum yields of corresponding processes presented in Fig. 3 is dictated by the spectral variation of the ratio between the surface concentration of electrons and holes [8,13].

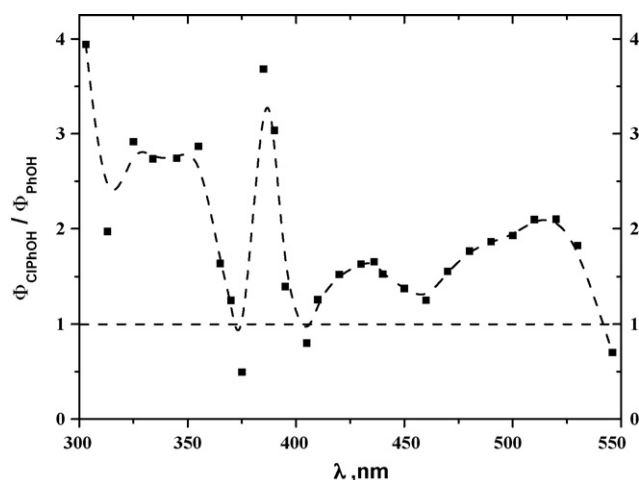
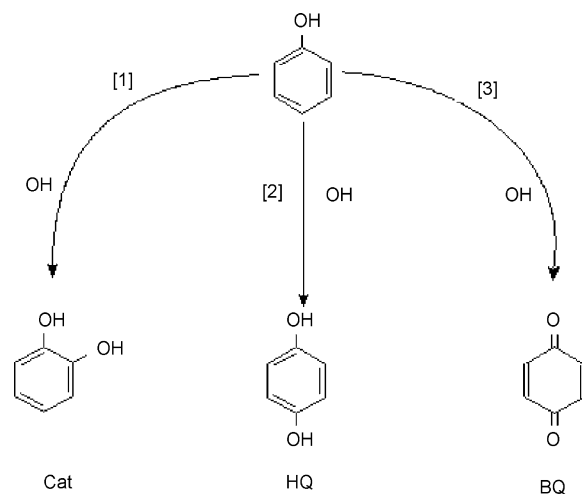


Fig. 3. Spectral variation of the ratio between the quantum yields of photodegradation of 4-chlorophenol and phenol over N-doped TiO₂.



Scheme 1. Formation of three major intermediates of phenol photodegradation (catechol, Cat; hydroquinone, HQ; benzoquinone, BQ) through interaction with photogenerated OH-radicals.

Note again that the spectral dependence of the ratio between corresponding quantum yields within the spectral range of fundamental absorption of TiO₂ is very similar to that observed for the pristine TiO₂ photocatalysts in both gas–solid and liquid–solid heterogeneous systems [8,32], that confirms our assumption that N-doping does not change significantly the band structure of TiO₂. At the same time, the spectral behavior of the ratio within the spectral region of the extrinsic N-doped induced light absorption is similar to the ratio between the quantum yields of photostimulated adsorption of oxygen and hydrogen, respectively, which is also proportional to the spectral variation of the ratio, e_s/h_s . Therefore, this similarity implies that observed spectral variation of the ratio between the quantum yields is an intrinsic feature of the N-doped TiO₂ sample and is governed by spectral variation of the ratio between the surface concentrations of electrons and holes, which depends on the migration properties of the charge carriers and spectral alteration of the mechanism of solid photoexcitation. In other words, the complex character of the spectral dependence of the ratio between the quantum yields of 4-chlorophenol and phenol photodegradation processes confirms the complex structure of the N-doped induced absorption in TiO₂. In turn, this conclusion denies the possibility of N-doped induced band-gap narrowing or formation of a new band of delocalized states within the band gap of TiO₂. Spectral dependences of the quantum yield and their ratio indicates the involvement of different localized states with different mechanisms of photoexcitation characterized by different values of the quantum yields of internal photoeffect in photoexcitation of N-doped TiO₂ within the spectral range of N-doped induced light absorption.

3.2. Spectral dependence of selectivity

As mentioned above, the phenol photodegradation occurs through the oxidation interaction with surface hole states (OH-radicals) only (see Scheme 1). To measure the spectral dependencies of the selectivity of N-doped TiO₂ we monitored the formation of three major intermediates: hydroquinone, benzoquinone, and catechol. Corresponding experimental spectral dependencies are presented in Fig. 4.

Since the photostimulated oxidation of phenol and formation of intermediates occur through interaction with OH-radicals, the

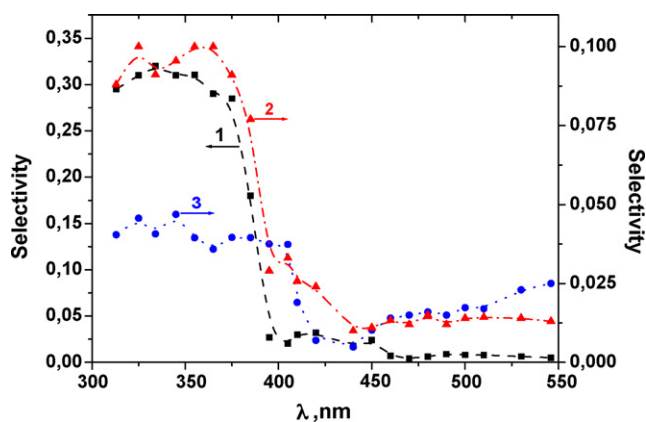


Fig. 4. Spectral variation of selectivity toward formation of hydroquinone (1), benzoquinone (2) and catechol (3) during phenol photodegradation over N-doped TiO₂.

expressions for the selectivity toward major intermediates can be written as:

$$S_{HQ} = \frac{d[HQ]/dt}{d[PhOH]/dt} = \frac{k_{HQ}[OH][PhOH]}{\sum_i k_i [OH][PhOH]} = \frac{k_{HQ}}{\sum_i k_i} \quad (10)$$

$$S_{BQ} = \frac{d[BQ]/dt}{d[PhOH]/dt} = \frac{k_{BQ}}{\sum_i k_i} \quad (11)$$

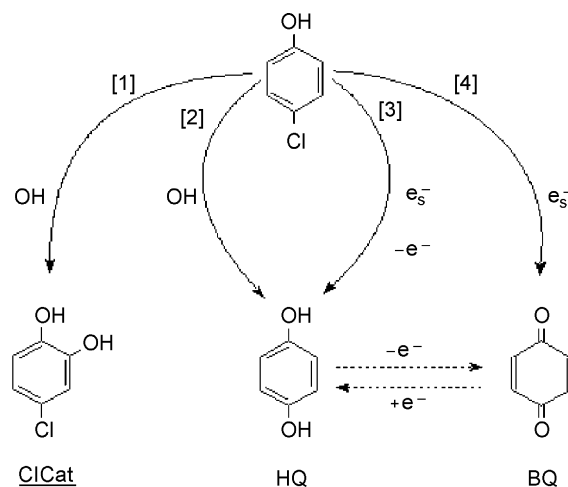
$$S_{Cat} = \frac{d[Cat]/dt}{d[PhOH]/dt} = \frac{k_{Cat}}{\sum_i k_i} \quad (12)$$

Thus, the selectivity of the photocatalyst does not depend on the concentration of photogenerated surface hole states (OH-radicals) and its spectral variation and should therefore be constant at different wavelengths provided that the type and mechanism of formation of the surface active sites remain the same. Such independence is observed for the fundamental absorption of TiO₂ regardless of the mechanism of band-to-band photoexcitation (indirect vs. direct). This result is in agreement with the spectral independence of selectivity measured for phenol photodegradation over pristine TiO₂ [13]. However, as is evident from the presented data, the selectivity of N-doped TiO₂ in visible spectral region is significantly different from that one in UV spectral region and demonstrates multi-step-like spectral variation. According to Eqs. (10)–(12) this behavior indicates an alteration of ratios between corresponding rate constants, that is, the surface active sites photogenerated at different wavelengths possess different thermodynamic properties and therefore different activities toward a particular reaction pathway. In other words, photoexcitation of N-doped TiO₂ at different wavelengths leads to formation of different surface active sites, which clearly indicates the difference in mechanisms of photoexcitation within N-doped induced absorption band caused by photoexcitation of localized states of different types.

In turn, photodegradation of 4-chlorophenol can process through both oxidation (interaction with surface hole states) and reduction (interaction with surface electron states) reaction pathways (see Scheme 2) resulting in formation of three major intermediates: hydroquinone, benzoquinone, and 4-chlorocatechol.

Corresponding experimental spectral dependencies of the selectivity of N-doped TiO₂ sample toward formation major intermediates are presented in Fig. 5.

According to the mechanism of 4-chlorophenol degradation presented in Scheme 2 the expressions for the selectivity toward



Scheme 2. Formation of three major intermediates of 4-chlorophenol photodegradation (chlorocatechol, ClCat; hydroquinone, HQ; benzoquinone, BQ) through interaction with photogenerated electrons and OH-radicals.

formation of the intermediates can be written as:

$$S_{HQ} = \frac{d[HQ]/dt}{d[ClPhOH]/dt} = \frac{(k_{HQ}[OH] + k'_{HQ}e)[ClPhOH]}{(\sum_i k_i [OH] + \sum_j k_j e) [ClPhOH]} = \frac{k_{HQ} + k'_{HQ}(e/h)}{\sum_i k_i + \sum_j k_j (e/h)} \quad (13)$$

$$S_{BQ} = \frac{d[BQ]/dt}{d[ClPhOH]/dt} = \frac{(k'_{BQ}e)[ClPhOH]}{(\sum_i k_i [OH] + \sum_j k_j e) [ClPhOH]} = \frac{k'_{BQ}(e/h)}{\sum_i k_i + \sum_j k_j (e/h)} \quad (14)$$

$$S_{ClCat} = \frac{d[ClCat]/dt}{d[ClPhOH]/dt} = \frac{(k_{ClCat}[OH])[ClPhOH]}{(\sum_i k_i [OH] + \sum_j k_j e) [ClPhOH]} = \frac{k_{ClCat}}{\sum_i k_i + \sum_j k_j (e/h)} \quad (15)$$

Thus, in addition to thermodynamic causes for selectivity (that is, generation of different surface active site characterized by different reaction rate constants), the spectral variation of the ratio between the surface concentrations of electrons and holes also play

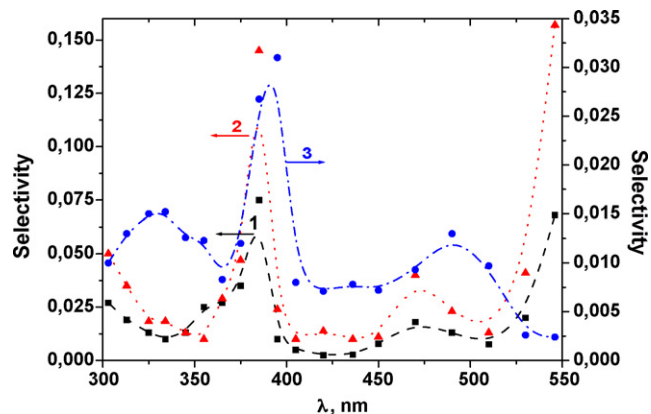


Fig. 5. Spectral variation of selectivity toward formation of hydroquinone (1), benzoquinone (2) and 4-chlorocatechol (3) during 4-chlorophenol photodegradation over N-doped TiO₂.

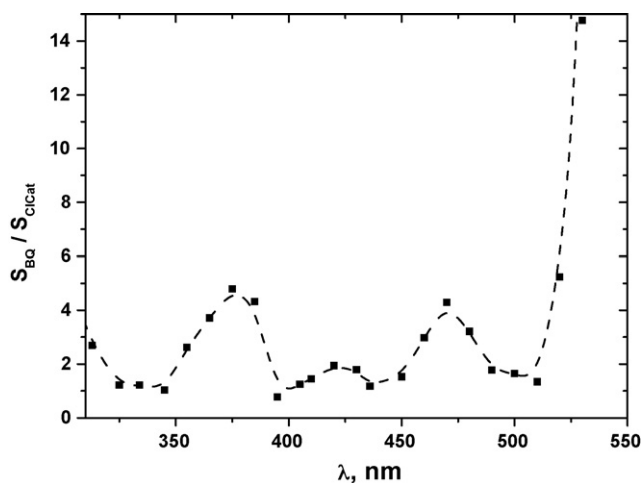


Fig. 6. Spectral variation of the ratio between the selectivities toward formation of benzoquinone and 4-chlorocatechol during 4-chlorophenol photodegradation over N-doped TiO₂.

a role in spectral selectivity of photocatalyst by changing the probability of oxidation and reduction reaction pathways. This results in more complex spectral variation of selectivity in 4-chlorophenol photodegradation compared to the selectivity of N-doped TiO₂ sample in phenol photodegradation where selectivity is dictated by thermodynamic factors only.

Note, that according to the Eqs. (14) and (15), the ratio between the selectivity of the photocatalyst toward formation of benzoquinone and 4-chlorocatechol (see Fig. 6) is proportional to the alteration between the surface concentrations of electrons and holes, which is dictated by the spectral variation of the selectivity of photocatalyst:

$$\frac{S_{BQ}}{S_{Cicat}} = A(\lambda) \left\{ \frac{e}{h} \right\} \quad (16)$$

Note that coefficient $A(\lambda)$ in turn can be spectrally variable provided the generation of different surface active states at different wavelengths reflecting the thermodynamic cause of the spectral selectivity of photocatalyst.

In spite of the complex nature of the reasons leading to the observed spectral dependencies of selectivity of N-doped TiO₂ sample, the position of the spectral features of the two different ratios dependent on the ratio between surface concentrations of electrons and holes and presented in Figs. 3 and 6 are in remarkable

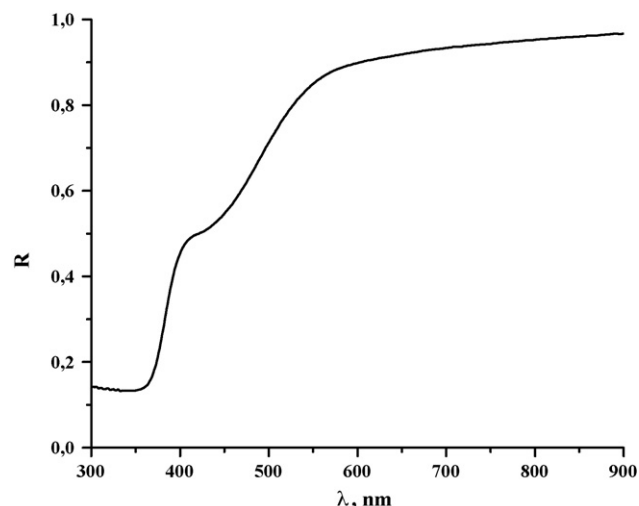
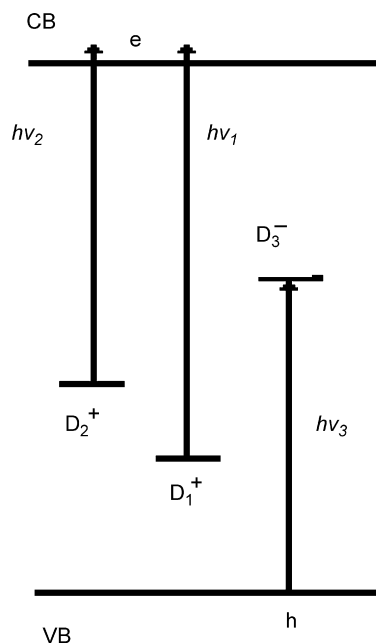


Fig. 7. Diffuse reflectance spectrum of the N-doped TiO₂ sample.



Scheme 3. Photoexcitation of localized (defect) states at the surface and/or in sub-surface space.

agreement. Again it clearly points at the different mechanisms of photoexcitation within N-doped induced absorption band inferring its complex composition caused by existence of the localized states of different type.

4. Conclusion

Fig. 7 represents the diffuse reflectance spectrum of the studied N-doped TiO₂ sample, which demonstrates broad unresolved N-doped induced absorption band in visible spectral region (typical for N-doped TiO₂).

From the experimental spectral dependencies of the quantum yield and selectivity of phenols photodegradation over N-doped TiO₂ we may deduce the existence of several single absorption bands forming the complex N-doping induced absorption spectrum within the spectral range of the extrinsic light absorption of the sample. Particularly, the band-like shape indicates the overlapping of dominating absorption bands with less active background, while the flat type dependence corresponds to the light absorption by a single absorption band. Consequently, such spectral features observed in spectral dependencies of the quantum yield of phenols photodegradation demonstrate the existence of three single absorption bands with maxima at about 420 nm, 450 nm, and 490–510 nm. In turn, spectral features of the ratio between the quantum yields of 4-chlorophenol and phenol photodegradation confirm the presence of absorption bands with maxima at 420–450 nm and 490–520 nm, which are responsible for the alteration of the ratio e_s/h_s .

In addition, the spectral dependencies of the selectivity of N-doped TiO₂ within spectral range of extrinsic light absorption toward formation of the selected major intermediates during phenol photodegradation shows the spectral features corresponding to generation of different surface active sites (see Scheme 3). According to the proposed simplified mechanism of N-doped TiO₂ photoexcitation of localized (defect) states at the surface and/or in sub-surface space with different wavelengths ($h\nu_1$ and $h\nu_2$) results in formation of different surface active centers possessing different selectivity.

Note, however, that the mechanism of photoexcitation of corresponding defects is similar, namely formation of positively charged states, D^+ , (trapped holes) which are able to initiate oxidation reaction, although with different product distribution caused by different ratios between corresponding rate constants in Eqs. (10)–(12). Thus, if two single absorption bands corresponding to photoexcitation of two different defects are overlapped, one can observe a step-like spectral dependence of photocatalyst selectivity—it remains nearly constant within spectral range of dominating light absorption by either single absorption band and drastically alters from one constant value of selectivity to another one within spectral range of significant overlapping of two bands. Consequently, analysis of the experimental spectral dependencies of the selectivity of N-doped TiO_2 in phenol photodegradation confirms the existence of the spectral features corresponding to different single absorption bands with maxima at about 420 nm, 440 nm, 490–500 nm.

At the same time, the spectral dependencies of the selectivity of N-doped TiO_2 for 4-chlorophenol photodegradation can be caused by, in addition to generation of different surface active centers of the same (either electron or hole) type with different selectivity, the alteration of the reduction and oxidation efficiencies due to alteration of the ratio between the surface concentrations of electrons and holes (see Scheme 3). Indeed, overlapping of two single bands ($h\nu_1$ and $h\nu_3$) with different mechanisms of photoexcitation of defect states results in spectral variation of the ratio between concentrations of electrons and holes at the surface and thus, in alteration of the relative efficiencies of reduction and oxidation processes. Corresponding experimental spectral dependencies of the selectivity of N-doped TiO_2 for 4-chlorophenol photodegradation indicate spectral features in absorption spectrum with maxima at 420, 460, and 490 nm. The same spectral features can be seen in the spectral dependence of the ratio between the selectivities of formation of benzoquinone and catechol, respectively. Therefore, summarizing the obtained results one can assume the existence of at least four different single absorption bands with maxima at 420 nm, 440–450 nm, 490 nm and perhaps, 510–520 nm forming the extrinsic absorption spectrum of N-doped TiO_2 . Note, that the positions of deduced maxima correspond well to those determined by measurement of the spectral dependencies of the quantum yield of oxygen and/or hydrogen photostimulated adsorption at N-doped TiO_2 in gas–solid heterogeneous systems [10]. They are also in good agreement with maxima of deconvolved single absorption bands in pristine and doped TiO_2 , which as assumed, belong to intrinsic defects (color centers) of TiO_2 [26]. Therefore, we can also assume that N-doping of TiO_2 leads to generation of additional intrinsic defects of TiO_2 to compensate the excess of negative charge of dopant anions, N^{3-} .

Hence, measurements of spectral dependencies of the quantum yields and selectivity of photochemical reactions in heterogeneous systems can be used as a spectroscopic tool to deconvolve otherwise complex absorption bands in solids. Moreover, using the proper reagent molecules with a certain pathway of electron transfer, one can establish the predominant mechanism of photoexcitation

within a given spectral range leading to generation of either electrons or holes or charge carriers of both types.

Acknowledgments

This study was supported by KAST and by a Grant-in-Aid from the Ministry of Education, Culture, Sports, Science and Technology (MEXT) of the Japanese Government. A.V.E. also thanks to Japanese Society for the Promotion of Science (JSPS) for long term fellowship.

References

- [1] A. Salinaro, A.V. Emeline, J. Zhao, H. Hidaka, V.K. Ryabchuk, N. Serpone, *Pure Appl. Chem.* 77 (1999) 321.
- [2] A.V. Emeline, N. Serpone, *Int. J. Photoenergy* 4 (2002) 91.
- [3] L.L. Basov, G.N. Kuzmin, I.M. Prudnikov, Yu.P. Solonitzyn, in: Th.I. Vilesov (Ed.), *Uspekhi Photoniki*. Iss. 6, LGU, Leningrad State University, 1977, p. 82.
- [4] V.N. Kuznetsov, A.A. Lisachenko, (*Zhurnal Fizicheskoi Khimii*) *Sov. J. Phys. Chem.* 65 (1991) 1568.
- [5] A.M. Volodin, (*Khimicheskaya Fizika*) *Russ. J. Chem. Phys.* 11 (1992) 1054.
- [6] A.V. Emeline, E.V. Lobytseva, V.K. Ryabchuk, N. Serpone, *J. Phys. Chem. B* 103 (1999) 1325.
- [7] A.V. Emeline, G.N. Kuzmin, D. Purevdorj, V.K. Ryabchuk, N. Serpone, *J. Phys. Chem. B* 104 (2000) 2989.
- [8] A.V. Emeline, A. Salinaro, N. Serpone, *J. Phys. Chem. B* 104 (2000) 11202.
- [9] A.V. Emeline, G.N. Kuzmin, L.L. Basov, N. Serpone, *J. Photochem. Photobiol. A: Chem.* 174 (2005) 214.
- [10] A.V. Emeline, G.N. Kuzmin, N. Serpone, *Chem. Phys. Lett.* 454 (2008) 279.
- [11] A.V. Emeline, V.K. Ryabchuk, N. Serpone, *J. Phys. Chem. B* 103 (1999) 1316.
- [12] A.V. Emeline, A.V. Frolov, V.K. Ryabchuk, N. Serpone, *J. Phys. Chem. B* 107 (2003) 7109.
- [13] A.V. Emeline, N. Serpone, *J. Phys. Chem. B* 106 (2002) 12221.
- [14] R. Asahi, T. Morikawa, T. Ohwaki, K. Aoki, Y. Taga, *Science* 293 (2001) 269.
- [15] S. Sakthivel, H. Kisch, *Chem. Phys. Chem.* 4 (2003) 487.
- [16] H. Irie, Y. Watanabe, K. Hashimoto, *J. Phys. Chem. B* 107 (2003) 5483.
- [17] S. Yin, H. Yamaki, M. Komatsu, Q. Zhang, J. Wang, Q. Tang, F. Saito, T. Sato, *J. Chem. Mater.* 13 (2003) 2996.
- [18] T. Lindgren, J.M. Mwabora, E. Avendano, J. Jonsson, C.-G. Granqvist, S.-E. Lindquist, *J. Phys. Chem. A* 107 (2003) 5709.
- [19] G.R. Torres, T. Lindgren, J. Lu, C.-G. Granqvist, S.-E. Lindquist, *J. Phys. Chem. B* 108 (2004) 5995.
- [20] O. Diwald, T.L. Thompson, T. Zubkov, Ed.G. Goralski, S.D. Walck, J.T. Yates Jr., *J. Phys. Chem. B* 108 (2004) 6004.
- [21] R. Nakamura, T. Tanaka, Y. Nakata, *J. Phys. Chem. B* 108 (2004) 10617.
- [22] M. Mrowetz, W. Balcerski, A.J. Colussi, M.R. Hoffmann, *J. Phys. Chem. B* 108 (2004) 17269.
- [23] S. Sakthivel, M. Janczarek, H. Kisch, *J. Phys. Chem. B* 108 (2004) 19384.
- [24] H. Fu, L. Zhang, S. Zhang, Y. Zhu, *J. Phys. Chem. B* 110 (2006) 3061.
- [25] C. Di Valentin, G.-F. Pacchioni, A. Selloni, *Phys. Rev. B* 70 (2004) 085116.
- [26] V.N. Kuznetsov, N. Serpone, *J. Phys. Chem. B* 110 (2006) 25203.
- [27] N. Serpone, *J. Phys. Chem. B* 110 (2006) 24287.
- [28] A.V. Emeline, N.V. Sheremetyeva, N.V. Khomchenko, V.K. Ryabchuk, N. Serpone, *J. Phys. Chem. C* 111 (2007) 11456.
- [29] X. Qiu, C. Burda, *Chem. Phys.* 339 (2007) 1.
- [30] A.V. Emeline, X. Zhang, M. Jin, T. Murakami, A. Fujishima, *J. Phys. Chem. B* 110 (2006) 7409.
- [31] A.V. Emeline, A.V. Rudakova, V.K. Ryabchuk, N. Serpone, *J. Phys. Chem. B* 102 (1998) 10906; A.V. Emeline, V.K. Ryabchuk, N. Serpone, *J. Photochem. Photobiol. A: Chem.* 133 (2000) 89; D.F. Ollis, *J. Phys. Chem. B* 109 (2005) 2439; A. Mills, J. Wang, D.F. Ollis, *J. Phys. Chem. B* 110 (2006) 14386.
- [32] A.V. Emeline, L.G. Smirnova, G.N. Kuzmin, L.L. Basov, N. Serpone, *J. Photochem. Photobiol. A Chem.* 148 (2002) 99.
- [33] U. Stafford, K.A. Gray, P.V. Kamat, *J. Catal.* 167 (1997) 25.
- [34] J. Theurich, M. Lindner, D.W. Bahnemann, *Langmuir* 12 (1996) 6368.
- [35] R.W. Matthews, D.F. Sangster, *J. Phys. Chem.* 69 (1965) 1938.